

## ASSESSING DROUGHT IMPACTS IN ERBIL, IRAQI KURDISTAN: A STUDY OF LAND SURFACE TEMPERATURE AND VEGETATION HEALTH INDEX USING LANDSAT TIME-SERIES

Ragheb K. Mohammad<sup>1,\*</sup>, Sara H. Zaki<sup>1</sup>, Heman A. Ahmed Gaznayee<sup>1,\*</sup>, Halmat A. Sabr<sup>1</sup>, Payman H. Aliehsan<sup>1</sup>, Sherwan Y. Hammad<sup>1</sup>, Snoor H. Ababakr<sup>2</sup>, Hawar A. Razvanchy<sup>2</sup>, and Kawa K. Hakzi<sup>2</sup>

<sup>1</sup> Department of Forestry, College of Agricultural Engineering Sciences, Salahaddin University, Erbil 44002, Kurdistan Region, Iraq.

<sup>2</sup> Department of Soil and Water, College of Agricultural Engineering Sciences, Salahaddin University, Erbil 44002, Kurdistan Region, Iraq.

\*Corresponding author email: [ragheb.mohammad@su.edu.krd](mailto:ragheb.mohammad@su.edu.krd)

\*Corresponding author email: [heman.ahmed@su.edu.krd](mailto:heman.ahmed@su.edu.krd)

Received: 12 Nov. 2024 Accepted: 14 Jan. 2024 Published: 24 Feb. 2025. <https://doi.org/10.25271/sjuoz.2025.13.1.1430>

### ABSTRACT:

Drought is a natural disaster that has severe implications for various aspects of society, including the economy, agriculture, environment, and community. The study conducted in the Erbil province, Kurdistan Region, Iraq from 1998 to 2017 aims to determine the frequency and intensity of drought, highlighting its diverse effects on society, encompassing the economy, agriculture, environment, and local community. Indicators, for instance, the Land Surface Temperature (LST) obtained from satellite data (Landsat) and the Vegetation Health Index (VHI), were employed to evaluate the severity of droughts. The outcomes indicated that Erbil encountered severe droughts in 1999, 2000, and 2008, which resulted in a significant decrease in crop outcomes. Additionally, 2008 was marked by escalating drought conditions, as measured by VHI values exceeding 40; as a result, the percentages reached (86.5%, 67.6%, and 53.7%), respectively. Significant relationships were revealed, with a confidence level of 0.9, between VHI and various factors such as precipitation, LST, and crop yield, with corresponding degrees of (-0.612, 0.615, 0.613, and 0.635). The study also disclosed that alterations and decreases in precipitation occur as the growing season progresses, whereas the following years (2000, 2008, and 2012) saw a pronounced decline in yield, failing to meet the lower limit of water demands for crops. Moreover, the most affected locations in Erbil Province were found to be in the central and southwestern parts of the province.

**KEYWORDS:** Erbil, Drought, Crops Yield, LST, VHI, Landsat Time Series.

### 1. INTRODUCTION

Drought, one of the most significant natural perils, has numerous adverse effects on human activity (Wang *et al.*, 2015). These include the decline of groundwater supplies, shrinkage of lakes and reservoirs, drinking water problems, and decreased supply of food and animal feed (Hameed, 2013; Al-Quraishi *et al.*, 2020). Cutting-edge technology, known as satellite remote sensing, has emerged, enabling the continuous collection of spatiotemporal information regarding Earth's surface (Almamalchy *et al.*, 2020; Gaznayee *et al.*, 2022). This approach is ideal for long-term and wide-area drought monitoring because of its wide monitoring span, high frequency, and short cycle (Song *et al.*, 2019). The above definitions serve as conceptual explanations that form the foundation for practical interpretation. The operational definition of drought aims to determine a specific region's commencement, conclusion, spatial extent, and severity, relying on scientific considerations (Leal Filho, 2011). Unlike other natural hazards, identifying a drought's exact onset and conclusion is challenging, and no single indicator or index can accurately predict its severity and onset. Moreover, the cumulative impacts of drought intensify over time, persisting from one season to another or even year to year (Lee *et al.*, 2017; Park *et al.*, 2019). Many contributing causes of droughts include extreme temperatures, severe winds, low humidity levels, rainfall patterns, and intensity during crop-growing seasons. In the Iraqi Kurdistan Region, for instance, climate change has resulted in a

significant decrease in precipitation, with the region receiving only half of its usual rainfall until 2007 (Fadhil, 2011; Al-Quraishi *et al.*, 2020). This decline in precipitation has adversely impacted agriculture and water supplies, leading to a drop in the water level, reduced river water levels, and drying up of springs. Assessing the condition of vegetation is often regarded as a crucial factor in understanding drought-related changes to the land surface. Drought causes the loss of moisture in plants, subsequently influencing vegetation growth and overall health (Gaznayee & Al-Quraishi, 2019). Various remote sensing indices have been developed to monitor vegetation. Insufficient water availability to meet the normal demands of users results in significant damage to plants and loss of crop yields (Wilhite, 2018). Several researchers have developed varied indices to assess, monitor, and map drought using indices created from remote sensing data combined with climatological parameters (Gaznayee *et al.*, 2022). Land Surface Temperature (LST) and vegetation indices have emerged as potential indicators of drought (Carlson *et al.*, 1990). Also, several studies have investigated the impact of drought stress on vegetation cover (Pei *et al.*, 2018; Qu *et al.*, 2019). A comparison between the vegetation drought index and crop production demonstrated that VHI is a suitable metric for tracking fluctuations in agricultural drought (Sholihah *et al.*, 2016). Researchers have shifted their attention to studying vegetation responses as an indirect means of monitoring drought stress (USAID, 2008; Walther, 2011). Mikail and Rahel (2023) utilized remote sensing (RS) and GIS-

\* Corresponding author

This is an open access under a CC BY-NC-SA 4.0 license (<https://creativecommons.org/licenses/by-nc-sa/4.0/>)

based techniques to evaluate the effectiveness of evidence-based belief function (EBF) and analytical hierarchy process (AHP) models for mapping flood-prone areas. The study also revealed employed GIS Pro 3.5 techniques alongside a modified Angström-Prescott equation to estimate the monthly average global solar radiation in the Erbil province based on latitude and daylight hours. The findings indicate that global solar energy in the region peaks at  $8.4 \text{ kW}\cdot\text{day}^{-1}\cdot\text{m}^{-2}$  during summer and drops to a minimum of  $1.6 \text{ kW}\cdot\text{day}^{-1}\cdot\text{m}^{-2}$  in winter. Erbil's choice as the focal point of this study was driven by two principal considerations. First, Erbil's vulnerability to drought is rooted in geographical position and climatic conditions. Consequently, thoroughly comprehending drought feature mapping and classification in this locale can advance anticipatory measures for future drought occurrences. Second, the three designated zones within Erbil showed considerable discrepancies in topography (VHI), which represents the Vegetation Health Index (LST), Land Surface Temperature, and rainfall distribution. This resulted in distinct variations in drought attributes observed across these three areas. The objective of this study is to examine the spatiotemporal patterns of drought severity to assess their impact on agriculture. These drought events have significantly affected the region's economic development and ecological environment. In addition, this study aimed to inspect the impact of decreased precipitation on vegetation stress and offer useful information to agricultural planners and regional policymakers. Given the low precipitation levels in Erbil

## 2. MATERIALS AND METHODS

### Study Site Description:

The study area was the Erbil Province is located in northern Iraq. This region encompasses two distinct physiographic units, mountainous terrain and foothills. Its geographical coordinates span from  $36^{\circ} 12' 11''$  to  $36^{\circ} 15' 10''$  north latitude and  $44^{\circ} 12' 11''$  to  $44^{\circ} 15' 10''$  E longitude. The elevation within the confines of Erbil fluctuated between 400 and more than 3000 m above the average sea level. Around an approximate area of  $15038.9 \text{ km}^2$ , the Erbil Province is comprised of ten districts and sub-districts: Mergasur, Choman, Kojsinjaq, Makhmur, Shaqlawa, (Soran; sub-district: Rawanduz), (Hawler; including sub-districts: Khabat and Dashti Hawler). As illustrated in Fig.1(B), Erbil's precipitation distribution demonstrates spatial variation, featuring an average annual rainfall of approximately 430 mm. Most of this precipitation was concentrated in the northern region. Considering its inherent environmental characteristics, Erbil can be classified into three well-defined zones: the Arid Zone (depicted by the red-coloured area), the middle arid zone, and the mountainous area in the northern part. The average annual precipitation in Erbil ranges from 250 mm in the southern portion of the city to over 1200 mm in the highlands bordering the Turkish and Iranian borders to the northeast (Karim *et al.*, 2018). The mean annual temperature in the region is approximately  $21^{\circ}\text{C}$ , with significant diurnal and annual temperature variations (UNESCO, 2009; UNISCO, 2014). The climate classification of the study area is categorized as Interior Mediterranean, characterized by mild winters and hot, dry summers (Saeed & Abas, 2012). Fig.1 shows how often it rains and snows, on average, in the Kurdistan area of Iraq. Generally, the Province experiences a Mediterranean climate, featuring cold and rainy winters and hot and dry summers. Evaporation in this region exceeds the annual rainfall. The United States Geological Survey (USGS) webpage provided access to Landsat raw data, and the months of April and May were the focus of this study. These months were chosen because of their association with the highest vegetation growth and proliferation rates. The acquired datasets comprised information from various satellites, encompassing vegetation, soil, and indices data. Before analysis, these datasets underwent preprocessing and digital processing to extract the relevant soil, vegetation cover, and LST information.

that very high to high flood hazard zones accounted for 32% of the area using the EBF method and 22% using the AHP method. Ibrahim (2024)

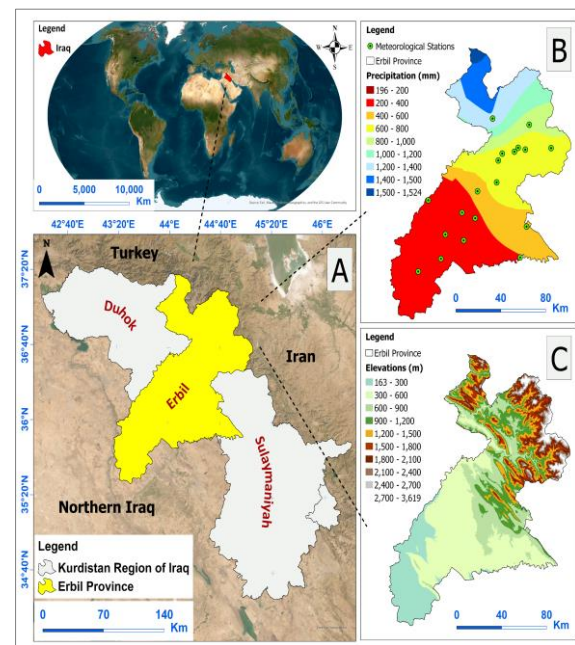


**Fig.1:** (A) Map of Iraq and Kurdistan region, (B) Study area is Erbil Province and meteorological stations, with annual rainfall (mm/year) 1997-2017, (C) Digital Elevation Map (DEM)

### Drought Spectral Indices Methodology:

**Gathering Data and Processing Digital Images:** We used various algorithms, such as VHI and LST, to extract information about vegetation cover and LST such as VHI and LST. Landsat data for April and May in the Erbil region were selected for this study. This choice was made because drought occurrences are more frequent during these months than during others, profoundly affecting crop yields.

**LST:** The Landsat thermal bands, mainly the 6th bands of Landsat 5 TM, Landsat 7 ETM+, and bands 10-11 of L8 TIRS, were utilized to extract fraction images of Land Surface Temperature (LST). Using the top of the atmospheric radiances obtained from the Thermal Infrared (TIR) sensor, the brightness temperature was calculated according to Planck's law. To obtain the brightness temperature, the U.S. The Geological Survey utilized TIR sensors and satellite datasets to calculate the top of atmospheric radiances, as mentioned by (Dash *et al.*, 2002). Five drought categories were then compared, and the one displaying the most significant deviation from the other four was selected as the dominant category. The percentages of land falling under each drought type were then tallied for each period to illustrate the temporal changes. The methodology documented by (Sun & Kafatos, 2007) was employed to convert digital numbers into land surface equations. The LST was calculated in Kelvin using the equation mentioned by Sun and Kafatos, 2007, and the conversion from Kelvin to Celsius was performed using Equation (1) stated by (HS, 2009). Different equations were utilized for the Landsat 5 and 7 bands to change the temperature of the thermal infrared band to ground temperature values, as mentioned by HS, (2009).

$$TB = K2 / \ln((K1 / L\lambda) + 1) \quad (1)$$

TB: brightness temperature in Kelvin (K)

$L\lambda$  is the Spectral Radiance at the sensor aperture (in  $\text{watts}/\text{m}^2 \times \text{ster} \times \mu\text{m}$ )

K1: band-specific thermal conversion constant (measured in  $\text{watts}/\text{m}^2 \times \text{srad} \times \mu\text{m}$ )

K2: represents the band-specific thermal conversion constant (measured in Kelvin)

One has seen the most significant shift compared to the other four categories. To show how the droughts progressed over time, the percentage of land affected by each type of drought was calculated for each timeframe.

The LST in Kelvin was measured using the following equation:

$$T = TB / [1 + (\lambda \times TB / \rho) \ln \epsilon] \quad (2)$$

where:  $\lambda$ : stands for the wavelength of emitted radiance,  $\rho = h \times c / \sigma$  ( $1.438 \times 10^{-2}$  m·K),  $h$  is Planck's constant ( $6.626 \times 10^{-34}$  J·s),

$\sigma$  = Boltzmann constant ( $1.38 \times 10^{-23}$  J/K),  $c$  = velocity of light ( $2.998 \times 10^{-8}$  m/s),

$\epsilon$  is the emissivity, given by the following equation:  $\epsilon = 1.009 + 0.047 \ln (\text{NDVI})$  by Sun and Kafatos, 2007.

The following equation measures Kelvin to Celsius:

$$T_c = T - 273 \quad (3)$$

where:  $T$  = LST value in Kelvin

$T_c$  = LST value in Celsius

Applying the following formulas, obtained from Landsat 5 and 7, allowed for the conversion of the temperature of the thermal infrared band into surface temperature values:

Convert DN value to radiance:

$$0.05518 \times (il) + 1.2378 \quad (4)$$

Convert radiance value to Kelvin:

$$1260.56 / \log ((666.09 / il) + 1) \quad (5)$$

Convert Kelvin value to Celsius:

$$i1 - 273.15 \quad (6)$$

where:  $il$ : stands for the reflectance of the thermal infrared band (HS, 2009).

**VHI:** The vegetation health index (VHI) has undergone additional development, as highlighted by several researchers (Du et al., 2013; Kogan, 2004; Kogan, 1990). This index was created to distinguish ecological factors from weather-related variables, specifically those associated with the NDVI components (Kogan, 1986). The Vegetation Condition Index is another equation that can be used to calculate another parameter. This equation uses NDVI measurements from the current month to define LST, where (NDVI min) and (NDVI max) represent the minimum and maximum NDVI values observed during the given interval, respectively. Although some researchers have advocated for the VHI to predict drought classification, relying solely on these values may offer an insufficiently precise description of drought conditions at any given location (Sahoo et al., 2015). VHI has seen further development through the incorporation of the following equations (Kogan, 1990; Kogan, 2004; Du et al., 2013):

$$VHI = 0.5 \times VCI + 0.5 \times TCI \quad (7)$$

The VCI was created to distinguish between NDVI's weather-related and ecological elements of NDVI (Kogan, 1986). The computation can be accomplished using Equation 2 in the following manner:

$$VCI = 100 \times \frac{(NDVI - NDVI_{min})}{(NDVI_{max} - NDVI_{min})} \quad (8)$$

$$TCI = 100 \times (T_{max} - T_c) / (T_{max} - T_{min}) \quad (9)$$

Equation 2 uses the term "NDVI" to refer to the NDVI score for the current month, with (NDVI min) standing for the lowest NDVI value and (NDVI max) for the highest NDVI value recorded throughout the monitoring period. Several researchers have recommended that the VHI as a drought tool, but the VHI values alone did not sufficiently describe the drought status (Kogan, 1986). Table 1 shows Kogan's classification of VHI levels based on droughts in the study region (Kogan, 1990; Du et al., 2013).

**Table 1:** Shows Kogan's classification of the VHI levels based on droughts in the study region (Kogan, 1990; Du et al., 2013)

Drought classification	Values
Extreme	$\leq 10$
Severe	$10 < & \leq 20$
Moderate	$20 < & \leq 30$
Mild	$30 < & \leq 40$
No Drought	$\geq 40$

### 3. RESULTS AND DISCUSSION

#### Vhi:

During the study period, this study examined vegetation health in the Erbil region and uncovered the influence of drought on its spatial patterns. Table 2 identifies 2000 and 2008 as the driest periods. Conversely, in 2002 and 2016, the vegetation health index exhibited the highest values with minimal drought-affected areas. Drought severity varied from mild to severe in these dry years, with an important portion of the study region enduring moderate-to-severe droughts. Figs. 2 and 3 effectively display the spatial distribution of drought events and severity categories, revealing that, although some small patches remained unaffected by drought, most of the study region experienced issues during these dry years. This study offers valuable insights into the spatial patterns of vegetation health and the consequences of drought in the Erbil region during the study period. These findings can help policymakers make well-informed decisions about managing water supply in the region and offer useful insights for developing efficient drought control methods. The results of the research, depicted in Table 2 and Figs. 2 and 3, elucidated the spatial patterns of vegetation health at the study site, which were significantly influenced by drought throughout the growing seasons of the two driest years (2000 and 2008) observed in Erbil throughout the study period. Table 2, presenting the VHI values, highlights that the smallest extent of the no-drought category (VHI > 40) was observed in the year 2000, covering a mere  $5.5 \text{ km}^2$  (0.5%) of the total area. In 2008, the area under the same drought category expanded to  $494.1 \text{ km}^2$  (9.3%) of the entire study area. In 2016, the highest VHI area, encompassing  $5,843.9 \text{ km}^2$ , accounted for 70.6% of the total area. The spatial distributions of drought events and severity categories for both dry and wet years are shown in Figs. 2 and 3. Drought severity ranged from mild to severe in 2000 and 2008 (Table 2). The maps (Figs. 2 and 3) clearly demonstrate that although 2000, 2008, and 2012 were categorized as years with low precipitation, certain isolated areas in northern Erbil remained untouched by drought. Nonetheless, intense drought conditions were widespread across the entire region during these arid years, with most areas facing varying degrees of moderate to severe drought. Erbil's northern and eastern regions have higher elevations and generally receive more rain each year. An approach for assessing drought conditions within a chosen region was provided by examining a number of drought indices. Fluctuations in the Vegetation Health Index (VHI) demonstrate that from April 2000 to 2008, there were notable stress and drought impacts on vegetation cover. The lower average precipitation and continuously high temperatures throughout these two years, which resulted in a decline in the VHI values, are responsible for this occurrence. The elevated LST observed during these periods, caused by limited precipitation and increased air temperature, further supports these findings. This correlation is evident in the VHI values. Consequently, LST and VHI can effectively detect and map the severity of droughts. These results are consistent with those reported previously (Bhuiyan et al., 2006).

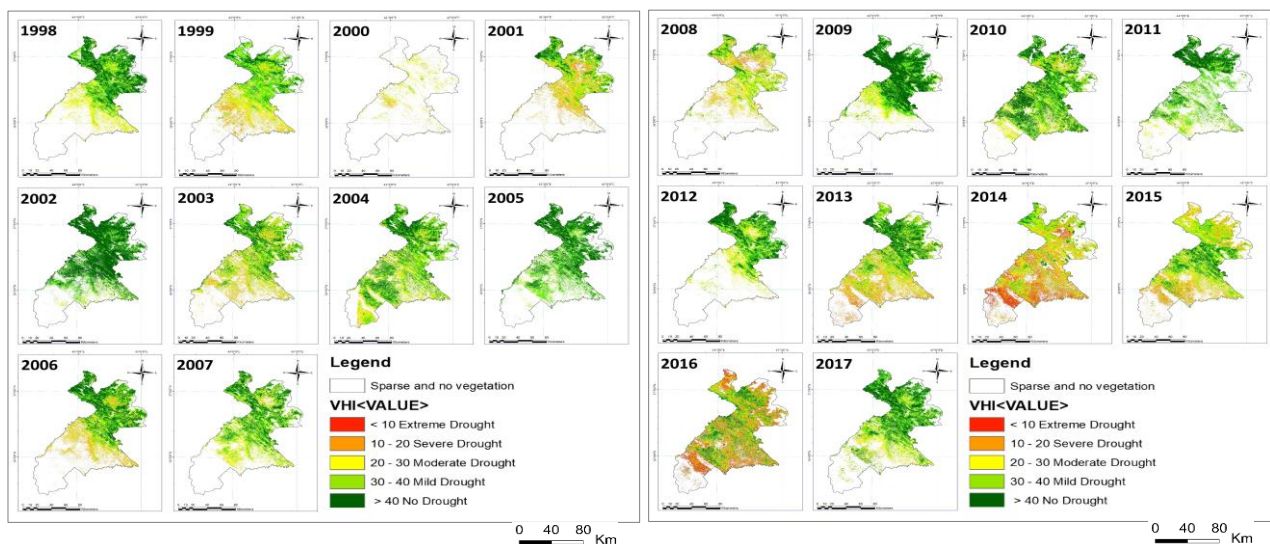


**Fig. 2:** Drought severity classification from 1998 to 2007 based on the VHI index

**Fig. 3:** Drought severity classification from 2008 to 2017 based on the VHI index

**Table 2:** Shows the area of the different levels of drought severity in Erbil Province from 1998 to 2017 based on the VHI

Year	Drought Classification									
	VHI <= 10 Extreme		10 < VHI <= 20 Severe		20 < VHI <= 30 Moderate		30 < VHI <= 40 Mild		VHI > 40 No Drought	
	Area [Km <sup>2</sup> ]	Area [%]								
1998	1,003.2	13.1	2,315.6	30.3	2,534.3	33.1	1,530.2	20.0	263.1	3.4
1999	1,046.1	13.8	2,400.4	31.7	2,789.9	36.8	1,187.6	15.7	151.7	2.0
2000	0.0	0.0	248.9	22.0	728.7	64.5	146.1	12.9	5.5	0.5
2001	81.4	1.4	1,387.8	23.4	1,866.3	31.5	1,507.0	25.4	1,085.5	18.3
2002	0.0	0.0	0.0	0.0	357.1	4.3	2,075.2	25.1	5,843.9	70.6
2003	1.4	0.0	1,287.4	15.8	2,512.5	30.9	2,408.5	29.6	1,914.5	23.6
2004	0.0	0.0	360.3	3.6	2,898.3	28.8	3,546.4	35.2	3,262.7	32.4
2005	0.0	0.0	0.0	0.0	489.3	6.9	2,933.3	41.1	3,711.0	52.0
2006	5.0	0.1	1,185.2	15.0	1,745.4	22.1	2,138.6	27.1	2,811.5	35.7
2007	0.0	0.0	198.7	2.6	2,386.3	31.2	2,772.3	36.3	2,278.8	29.8
2008	99.0	1.9	1,410.9	26.7	2,164.3	40.9	1,125.3	21.3	494.1	9.3
2009	0.0	0.0	409.0	5.4	1,625.5	21.7	2,535.5	33.8	2,935.3	39.1
2010	3.5	0.0	303.6	3.0	2,412.3	23.6	3,441.0	33.7	4,054.2	39.7
2011	0.0	0.0	0.4	0.0	934.7	15.1	2,798.7	45.1	2,467.5	39.8
2012	0.0	0.0	888.9	13.4	2,216.0	33.5	2,050.6	31.0	1,468.7	22.2
2013	254.9	2.7	2,142.4	22.5	2,413.8	25.3	2,483.7	26.1	2,227.8	23.4
2014	1,715.2	17.9	2,783.0	29.0	2,854.5	29.8	1,685.7	17.6	553.1	5.8
2015	65.9	0.7	2,079.1	22.1	3,107.7	33.0	2,735.0	29.0	1,439.0	15.3
2016	2,003.2	19.5	2,113.6	20.5	2,257.0	21.9	2,034.3	19.8	1,884.0	18.3
2017	0.0	0.0	206.1	2.5	1,938.5	23.2	2,842.9	34.1	3,352.2	40.2

The study analyzed VHI maps' work in depth, indicating that plant growth depends on water supply through rainfall and irrigation (Bhuiyan, 2004). This study provides valuable insights into the spatial patterns of vegetation health and the impact of drought in the Erbil region during the study period. These findings can inform drought management strategies and help policymakers make informed decisions regarding water resource management in this region. As an early warning system, the VHI is one of the most vital indicators for monitoring the onset of drought stress (Bhuiyan, 2004). The southern areas are more exposed to severe drought due to low vegetation cover values and annual rainfall (Wan *et al.*, 2004). Droughts are complex phenomena in their origin, as they are linked to a combination of topographic, atmospheric, and hydrological elements that collectively impact soil moisture and plant growth (Vogt *et al.*, 1998). The vegetation cover in Erbil has remained relatively consistent over the past decade, with notable exceptions in 2000, 2008, and 2012. The convergence of factors, including the region's low altitude and high latitude, accompanied by a decline in yearly precipitation and elevation in Land Surface Temperature (LST), could be attributed to the primary drivers behind this occurrence. The explanation is that the southern

sectors of Erbil are characterized by unusual rainfall, with annual precipitation not exceeding 200 mm. High temperatures in April cause fluctuations in the amount of rain, which stresses plants and increases the evaporation of crops grown in such location. According to the VHI and LST maps, the Erbil Plain was classified under drought conditions, particularly in 2000, 2008, and 2012 (Figs. 2, 3, 4, 5, and 6). The decline in crop area, yield, and agricultural land is an issue of great concern (Table 5). The rise in temperature and decrease in rainfall have significantly affected crop area and yield, adversely affecting agriculture in the region. The southern areas of Erbil Province bear the brunt of this impact, receiving minimal rainfall, with annual totals not exceeding 200 mm. For crops growing in these specific areas, unpredictable precipitation in April and high temperatures increases the stress on plants and the process of evaporation. It is imperative to address these challenges and implement measures to mitigate the impacts of climate change in the region. This could involve implementing water conservation initiatives. In contrast, Erbil's LST in 2000 and 2008 were approximately 38°C and 37°C, respectively. In general, the southern parts of the

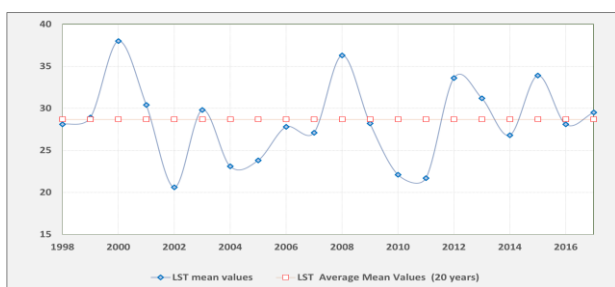


**Fig.4:** Shows the mean of annual LST values for the study site (Erbil) between 1998 to 2017

This temperature disparity can be largely attributed to factors such as lower precipitation, limited vegetation cover, and lower elevation in these areas. The southern regions consistently encountered elevated temperatures in comparison to the northern regions because of these contributing factors. The Land Surface Temperature (LST) map further illustrates the trend of temperature escalation from the northeastern region toward the southwestern part. Mountainous areas exhibited relatively lower temperatures, whereas plains experienced higher temperatures. Vegetation cover affected LST, while areas with low rainfall and bare soil tended to have higher temperatures. Furthermore, the study area has experienced periods of drought, with some areas in the southern part of Erbil being hit by severe and very severe droughts during dry years. The drought severity levels in Erbil Province from 1998 to 2017, their area values presented in square kilometers and their percentages are shown in Table 3. These drier periods were divided into five different groups. Interestingly, the three years 2002, 2008, and 2012 experienced the worst drought conditions, which were marked by temperatures above 40 °C. Regarding the intensity of the drought, these years were categorized as being in category five. The severe character of the droughts in those particular years is highlighted by this classification. Statistically, LST was negatively correlated with the VHI, indicating that areas with better vegetation growth tended to have lower LST. (Figs 5 and 6), respectively. The lower part of the LST map (in red color Class 5 > 40 °C) of the study

study area had higher temperatures, enhancing irrigation techniques, and promoting the cultivation of drought-resistant crops.

#### Lst:

Fig. 4 illustrates the LST conditions in the research area from 1998 to 2017. The procedure involved comparing the average Land Surface Temperature (LST) values for each year within the research timeframe with the average LST over the course of 20 years in Erbil Province from 1998 to 2017. Erbil's temperature gradually increased; however, between 20°C (2002) and 22°C (2010), there was a declining trend.

area had a lower temperature than the middle part (in orange color Class 4, 30-40 °C). However, the lower part has an altitude is lower than the middle part, and characterized by low annual rainfall (Figs 5 and 6). In addition, the soils of that area tend to be bright in color in most places. In terms of statistical analysis, there were noteworthy negative correlations between the LST and VHI, as shown in Table 2. Reduced evapotranspiration on the shaded side is vital in promoting vegetation growth, especially within mountains in semi-dry regions (Wan *et al.*, 2004). Remarkably, the study site is situated within a semi-dry area, leading to a similar correlation between the aspect ratio and vegetation cover. Conversely, the study investigated temperature fluctuations within the region. Essentially, there is a gradient from the northeast to the southwest, where temperatures rise while vegetation cover diminishes. For instance, areas with the highest Land Surface Temperature (LST) values (>40°C) also presented extremely low vegetation cover, as indicated by the Vegetation Health Index (VHI), whereas regions with LST values ranging from 30 to 40°C showed dense vegetation cover. Numerous environmental factors, including topography, temperature, precipitation, and their collective influence on climate, significantly control vegetation cover. The first step in validating the results was to conduct field visits to randomly chosen locations in the study area. These locations were georeferenced to ensure their placement accuracy.

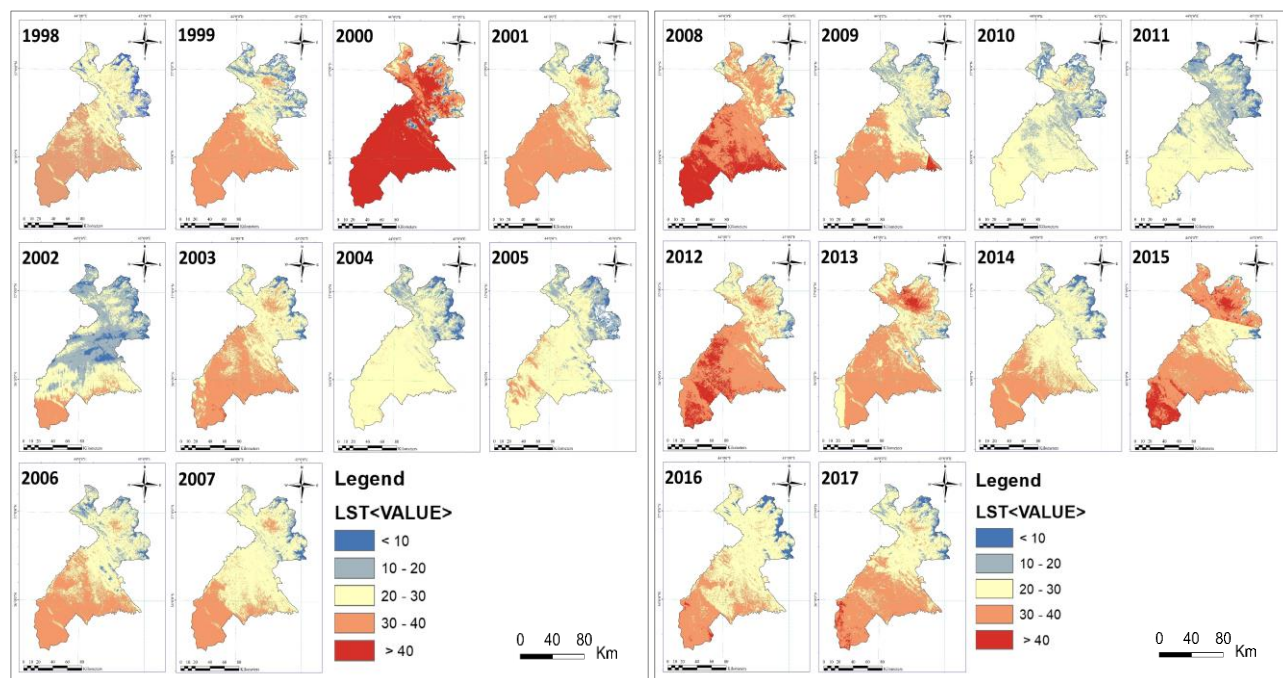


**Fig. 5:** Drought severity classes in Erbil from 1998 to 2007, based on the LST index

**Fig. 6:** Drought severity classes in Erbil from 2008 to 2017, based on the LST index

**Table 3:** Shows drought severity zones in the Erbil Province based on the LST Index, and LST classification calculated from Landsat Thermal Bands from 1998 to 2017

Year	Category 1 < 10 °C		Category 2 10-20 °C		Category 3 20-30 °C		Category 4 30-40 °C		Category 5 > 40 °C	
	Area (Km <sup>2</sup> )	Area (%)								
1998	370.5	2.5	1,219.7	8.2	6,060.0	40.9	7,100.6	47.9	67.3	0.5
1999	602.4	4.1	1,585.2	10.7	4,110.5	27.7	8,514.6	57.5	5.4	0.0
2000	328.9	2.2	235.8	1.6	857.0	5.8	2,763.7	18.7	10,632	71.8
2001	203.8	1.4	999.6	6.7	4,630.1	31.2	8,949.2	60.4	35.4	0.2
2002	1,331.3	9.0	6,085.5	41.1	5,523.4	37.3	1,800.7	12.2	77.3	0.5
2003	295.4	2.0	597.0	4.0	6,209.0	41.9	7,684.0	51.9	32.7	0.2
2004	596.8	4.0	2,221.0	15.0	11,890	80.2	86.7	0.6	23.4	0.2
2005	665.5	4.5	2,264.5	15.3	10,617	71.7	832.7	5.6	438.1	3.0
2006	261.0	1.8	1,523.7	10.3	6,621.9	44.7	6,406.0	43.2	5.5	0.0
2007	254.7	1.7	973.7	6.6	9,302.6	62.8	4,280.1	28.9	7.0	0.0
2008	164.2	1.1	407.8	2.8	2,203.1	14.9	7,366.0	49.7	4,677.1	31.6
2009	311.5	2.1	2,190.5	14.8	5,605.7	37.8	6,560.9	44.3	149.6	1.0
2010	593.3	4.0	3,341.9	22.6	10,408	70.2	474.5	3.2	0.0	0.0
2011	743.2	5.0	4,259.3	28.7	9,695.1	65.4	120.5	0.8	0.0	0.0
2012	143.6	1.0	124.0	0.8	3,115.7	21.0	8,192.2	55.3	3,242.6	21.9
2013	128.5	0.9	367.5	2.5	4,809.5	32.5	9,050.4	61.1	462.2	3.1
2014	516.5	3.5	1,269.7	8.6	7901.7	53.3	5,101.8	34.4	28.5	0.2
2015	162.1	1.1	193.7	1.3	4,150.9	28.0	9,437.9	63.7	873.5	5.9
2016	539.4	3.6	469.9	3.2	8,992.5	60.7	4,742.9	32.0	73.5	0.5
2017	317.8	2.1	1,077.5	7.3	6,283.5	42.4	6,876.1	46.4	263.2	1.8

To determine the best vegetation index, several locations with low vegetation cover were selected and placed on all vegetation index maps using ArcMap. The values of reflectance number (DN) were then taken from all vegetation index maps for the same locations and compared to one another. VHI was a prominent indicator among the evaluated vegetation indicators, and the findings were supported through field validation. Nearly half of the cultivated wheat and barley crops suffered losses, primarily due to agricultural drought. We can infer from Fig. 5, that the severe agricultural drought in 2008 caused substantial crop damage, leading to a significant drop in crop yield. Based on a comprehensive analysis, satellite remote sensing has emerged as a viable approach for monitoring agricultural drought. Within the range of indices discussed in this study, LST and VHI, combining the Vegetation Condition Index (VCI) and Temperature Condition Index (TCI), exhibit higher spatial resolution. Primarily, the most affected areas lie in the southern part of Erbil, situated within the southern region of the broader Erbil area, where extreme drought conditions are prevalent.

#### Correlation Matrix Statically Analysis:

Rainfall is a key factor influencing vegetation growth, providing the necessary moisture for plants to grow and thrive. A lack of rainfall can lead to drought, which can cause vegetation stress and even death. Several factors, including the amount of vegetation cover, land cover type, and soil moisture in the soil, influence LST. A positive correlation exists between rainfall and VHI because increased rainfall typically leads to increased vegetation growth and health. However, the relationship between rainfall and LST is more complex. Table 4, shows understanding the connection between rainfall, VHI, and LST within a study area is crucial for discerning the well-being and productivity of vegetation in that region and evaluating the influence of different environmental factors. Significant positive correlations emerged between the Vegetation Health Index (VHI) and precipitation ( $r=0.615^{**}$ ) and between VHI and crop yield ( $r=0.613^{**}$ ), while negative correlations were observed between VHI and LST ( $r=-0.612^{**}$ ), and between VHI and Class 5 LST ( $r=-0.800^{**}$ ).

**Table 4:** The relationship coefficients between precipitation, crop area, crop yield, and the spectral indicators.

	VHI	LST	Precipitation (mm)	Crop Yield (ton)	Crop Area (km <sup>2</sup> )	Class 5 (LST)	
VHI	1	-0.612**	0.615**		0.613**	0.105	-0.800**
LST	-0.612**	1	-0.456*		-0.407	-0.197	0.790**
Precipitation (mm)	0.615**	-0.456*	1		0.604**	0.212	-0.505*
Crop Yield (ton)	0.613**	-0.407	0.604**		1	0.486*	-0.486*
Crop Area (km <sup>2</sup> )	0.105	-0.197	0.212		0.486*	1	-0.143
Class 5 (LST)	-0.800**	0.790**	-0.505*		-0.486*	-0.143	1

2-tailed - correlation with two stars (\*\*) are significant at the 0.01 level

2-tailed - correlation with one star (\*) are significant at the 0.05 level

The mountainous terrains characterized by higher elevations approximately more than 3,000 m a.s.l (Razvanchy, 2008). expand in a northeast-to-southwest orientation, regularly diminishing towards the southwest. From a statistical perspective, meaningful, significant relationships were identified between rainfall, VHI, and LST indices. Moreover, in 2000 and 2008, a higher LST was observed, which could be caused by a lack of precipitation and high air temperature. The VHI numbers clearly demonstrate this drop. VHI can accurately identify and map the severity of droughts. The study analysed VHI maps, which showed that while plant growth depends on water availability from rain and irrigation, it can endure unfavourable hydrological and meteorological conditions over several seasons (Sahoo et al., 2015). The southern parts of Erbil Province are more vulnerable to severe drought because of the low vegetation

cover and annual rainfall. These features could indicate relatively low vegetation cover and photosynthetic activity, which causes slight temporal variations (Zhang et al., 2019). Across the studied timeframe, the southern region of Erbil Province displayed a notable rise in Land Surface Temperature (LST). This elevation in LST seems to be linked to land degradation induced by droughts, a problem in this area. The origins of droughts are complicated because of their connection to atmospheric, topographic, and hydrological elements that influence soil moisture and vegetation growth (Sutcliffe, 2012). The highest VHI values in this study were observed in the northern region, which was associated with the highest Precipitation and higher elevations. The statistical relationship between rainfall and VHI was significantly positive in this study, also reported by (Sutcliffe, 2012). The results presented in Table 5 show a

substantial inverse relationship between VHI and LST ( $r = -0.937$ ). A positive relationship ( $r=0.909$  and  $0.827$ ) existed between the VHI with elevation and precipitation. However, the relationship between LST, DEM, precipitation, and VHI was negative ( $r = -0.913, -0.890$ , and  $-0.937$ ). The correlation Matrix

between precipitation, elevation, VHI, and LST and the mean for the 20 sub-district locations are presented in Table 5 and Fig.7. A statistically significant relationship existed between the remote sensing-based spectral indicators and precipitation.

**Table 5:** Relationship coefficients between precipitation, correlation matrix values between elevation (m) and precipitation (mm), and spectral indicators.

	DEM (m)	Precipitation (mm)	LST	VHI
<b>DEM (m)</b>	1	0.881	-0.913	0.909
<b>Precipitation (mm)</b>	0.881	1	-0.890	0.827
<b>LST</b>	-0.913	-0.890	1	-0.937
<b>VHI</b>	0.909	0.827	-0.937	1

Bold numbers indicate differences from 0 with a significance level of alpha = 0.05

### Multiple Linear Regression Statically Analysis:

Rainfall has a significant impact on vegetation growth because it gives plants the moisture they need to develop and flourish. Drought conditions brought on by insufficient rainfall can stress or even kill plants. The land surface temperature (LST) is a measurement that depends on several elements such as the kind and quantity of vegetation cover as well as the soil's moisture content. Rainfall and plant health are positively correlated because higher rainfall generally promotes healthier and more vegetative growth. Rainfall and LST have a more complicated relationship because more rainfall might result in

more soil moisture and a drop in surface temperature, which can also lead to increased vegetation cover, which can cause a reduction in surface temperature. Fig.7 illustrates the geographic distributions of variations in elevation, precipitation, LST, and VHI in the 20 sub-districts of the Erbil Province. This suggests that while LST significantly increased, rainfall and VHI significantly decreased in the south. Despite knowing that fluctuations in LST and NDVI were observed in the study locations, there were considerable decreases in LST noted in the northern region of the country that were driven by higher elevations and VHI values.

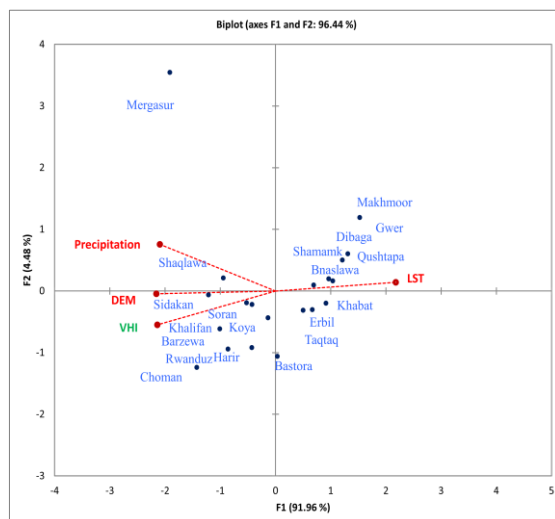


**Fig.7:** Alterations in the spatial patterns of ecological parameters and drought indices were examined for 20 years across 20 locations.

The relationship between seasonal fluctuations in vegetation output and environmental variables was examined using a multiple regression analysis. Many studies have used these analyses to quantify variability in vegetation dynamics over time and space (Busetto *et al.*, 2010; Jiao *et al.*, 2016; Guo *et al.*, 2017). A spatiotemporal relationship model was developed to determine the long-term responses of VHI and LST related to environmental variables.

Table 6 shows the multiple regression statistics used to determine the significance of the ecological parameters of the regression models used to predict drought indicators in Erbil. The results of the LST module were ( $R^2 = 0.865$ ), (RMSE= 1.486), (MSE=2.209), and (MAPE=4.182). However, the values of the VHI (module 1) were as follows: ( $R^2 = 0.829$ ), (RMSE= 3.5), (MSE=12.25), and (MAPE=8.42). The regression models highlighted the complex interactions among elevation, rainfall, LST, and VHI. Elevation appeared to have significantly influenced both the LST and VHI values, whereas rainfall exhibited varying effects on different modules of the VHI. Moreover, LST demonstrated its impact on VHI in Module 2.

**Table 6:** Regression model variables were applied in Erbil province to forecast indices of drought (LST and VHI).

Index	R <sup>2</sup>	RMSE	MSE	MAPE	Module Equation
LST Module	0.865	1.486	2.209	4.182	$LST=34.0229-7.5890E-03*Elevation-5.1742E-03*Rainfall$
VHI Module1	0.829	3.500	12.252	8.427	$VHI=18.8396+2.2214E-02*Elevation+3.2794E-03*Rainfall$
VHI Module2	0.899	2.768	7.662	5.064	$VHI=70.2359+1.075E-02*Elevation-4.5369E-03*Rainfall-1.51063*LST$

(RMSE) stands for Root Mean Square Error

(MSE) stands for Mean Squared Error

(MAPE) stands for Mean Absolute Percentage Error

The most significant drop in crop yield occurred in 2000 and 2008, primarily because of agricultural drought incidents (Table 7). This decline can be related to fluctuations in the amount of precipitation necessary to meet the minimum water demand of crops (Gaznayee & Al-Quraishi, 2019; Gaznayee, 2020). Typically, there is a correlation between crop yield, Vegetation

Health Index (VHI), and Land Surface Temperature (LST); this observation could serve as a foundation for establishing a connection between indices and crop yield. Furthermore, the average precipitation levels were reduced during the three years of drought, leading to a noticeable reduction in VHI values.

**Table 7:** Shows the study area's average crop area (Km<sup>2</sup>), crop yield (ton), and yearly precipitation (mm) over a 20-year period.

Years	Average Annual Precipitation (mm)	Crop Area (Km <sup>2</sup> )	Crop Yield (ton)
1997-1998	484.0	664.6	152,880.5
1998-1999	258.5	539.7	54,215.7
1999-2000	302.1	752.3	92,525.6
2000-2001	471.8	687.4	162,442.9
2001-2002	607.5	970.4	331,701.7
2002-2003	695.1	953.8	249,196.3
2003-2004	648.3	1,142.6	268,636.3
2004-2005	538.9	1,209.8	340,220.5
2005-2006	583.7	1,477.7	303,956.6
2006-2007	582.5	1,503.8	535,975.2
2007-2008	243.7	1,264.0	15,031.0
2008-2009	332.0	1,521.6	37,3951.6
2009-2010	529.8	1,225.3	354,899.3
2010-2011	454.6	1,364.2	257,135.0
2011-2012	389.9	628.8	101,292.0
2012-2013	690.8	636.8	319,856.0
2013-2014	435.8	132.9	337,224.0
2014-2015	537.2	1,491.2	448,869.0
2015-2016	659.0	1,380.1	601,396.0
2016-2017	428.4	949.0	411,676.0

## CONCLUSIONS

This paper outlines a study on tracking droughts (LST and VHI) over 20 years in Iraq's Erbil Province using satellite imagery and geographic information systems. The findings of this study show that the southern region of Erbil Province has experienced three consecutive years of drought, which is attributed to a decrease in annual rainfall, rising temperatures, and increased evapotranspiration caused by high wind speeds, high temperatures, and low relative humidity. Elevation was a significant factor affecting the variables in the study, particularly vegetation cover. The study also found a significant correlation between Landsat-based spectral drought indices, precipitation, and elevation. The correlations between the elevation and precipitation with the VHI and LST were strong. This study has important implications for policymakers in the KRI-Erbil to examine and evaluate drought-stricken areas. Based on research findings, the southern regions of Erbil Province have been experiencing drought due to a combination of factors, including a decrease in annual rainfall, rising temperatures, and increased evapotranspiration caused by high wind speeds, high temperatures, and low relative humidity. This study provides valuable insights into applying satellite imagery and GIS to drought monitoring. Future studies should have higher spatial and temporal resolutions to enhance drought monitoring accuracy.

### Acknowledgements:

The authors express their gratitude to the Forestry Department, College of Agricultural Engineering Sciences, Salahaddin University (SU), Erbil, Iraqi Kurdistan Region. The authors also extend their appreciation to the Ministry of Agriculture and Water Resources for their valuable support and assistance.

### Author Contributions

All authors contributed to the design and execution of this study. **R.K.M.**, and **H.A.A.G.**, led the manuscript review. **S.H.Z.**, and **H.A.S.**, contributed to methodology and investigation. **P.H.A.**, and **S.Y.H.**, performed data curation and formal analysis. **S.H.A.**, and **H.A.R.**, handled resources. **K.K.H.**, software and visualization. All authors have read and approved the final manuscript.

### Ethical Statement

This manuscript does not require ethical approval, as no human or animal experimentation was conducted.

## REFERENCES

Al-Quraishi, A. M. F., Qader, S. H., & Wu, W. (2020). *Drought monitoring using spectral and meteorological based indices combination: a case study in Sulaimanyah, Kurdistan region of Iraq*. Environmental remote sensing and GIS in Iraq, 377-393. [http://dx.doi.org/10.1007/978-3-030-21344-2\\_15](http://dx.doi.org/10.1007/978-3-030-21344-2_15)

Almamalachy, Y. S., Al-Quraishi, A. M. F., & Moradkhani, H. (2020). *Agricultural drought monitoring over Iraq utilizing MODIS products*. Environmental remote sensing and GIS in Iraq, 253-278. [http://dx.doi.org/10.1007/978-3-030-21344-2\\_11](http://dx.doi.org/10.1007/978-3-030-21344-2_11)

Bhuiyan, C. (2004). *Various drought indices for monitoring drought condition in Aravalli terrain of India*. Proceedings of the XXth ISPRS Congress, Istanbul, Turkey. <http://dx.doi.org/10.1016/j.jag.2006.03.002>

Bhuiyan, C., Singh, R., & Kogan, F. (2006). *Monitoring drought dynamics in the Aravalli region (India) using different indices based on ground and remote sensing data*. International Journal of Applied Earth Observation and Geoinformation, 8(4), 289-302. <https://doi.org/10.1016/j.jag.2006.03.002>

Busetto, L., Colombo, R., Migliavacca, M., Cremonese, E., Meroni, M., Galvagno, M., Rossini, M., Siniscalco, C., Morra Di Cella, U., & Pari, E. (2010). *Remote sensing of larch phenological cycle and analysis of relationships with climate in the Alpine region*. Global change biology, 16(9), 2504-2517. <https://doi.org/10.1111/j.1365-2486.2010.02189.x>

Carlson, T. N., Perry, E. M., & Schmugge, T. J. (1990). *Remote estimation of soil moisture availability and fractional vegetation cover for agricultural fields*. Agricultural and Forest Meteorology, 52(1-2), 45-69. [https://doi.org/10.1016/0168-1923\(90\)90100-K](https://doi.org/10.1016/0168-1923(90)90100-K)

Dash, P., Götsche, F.-M., Olesen, F.-S., & Fischer, H. (2002). *Land surface temperature and emissivity estimation from passive sensor data: Theory and practice-current trends*. International Journal of Remote Sensing, 23(13), 2563-2594. <https://doi.org/10.1080/01431160110115041>

Du, L., Tian, Q., Yu, T., Meng, Q., Jancso, T., Udvardy, P., & Huang, Y. (2013). *A comprehensive drought monitoring method integrating MODIS and TRMM data*. International Journal of Applied Earth Observation and Geoinformation, 23, 245-253. <https://doi.org/10.1016/j.jag.2012.09.010>

Fadhil, A. M. (2011). *Drought mapping using Geoinformation technology for some sites in the Iraqi Kurdistan region*. International Journal of Digital Earth, 4(3), 239-257. <https://doi.org/10.1080/17538947.2010.489971>

Gaznayee, H. (2020). *Modeling Spatio-Temporal Pattern of Drought Severity Using Meteorological Data and Geoinformatics Techniques for the Kurdistan Region of Iraq Agriculture Science (Application of GIS and Remote Sensing in Drought)*. Salahaddin University-Erbil, Sulaimani, Iraq. <http://dx.doi.org/10.13140/RG.2.2.17234.30402>

Gaznayee, H. A., & Al-Quraishi, A. M. F. (2019). *Analysis of agricultural drought's severity and impacts in Erbil Province, the*

Iraqi Kurdistan region based on time series NDVI and TCI indices for 1998 through 2017. *Jour of Adv Research in Dynamical & Control Systems*, 11(11), 287-297. <https://doi.org/10.5373/JARDCS/V11I11/20193198>

Gaznayee, H. A. A., & Al-Quraishi, A. M. F. (2019). Analysis of agricultural drought, rainfall, and crop yield relationships in Erbil Province, the Kurdistan region of Iraq based on Landsat time-series MSAV12. *J. Adv. Res. Dyn. Control Syst*, 11(12), 536-545. <https://doi.org/10.5373/JARDCS/V11SP12/20193249>

Gaznayee, H. A. A., Al-Quraishi, A. M. F., Mahdi, K., & Ritsema, C. (2022). A geospatial approach for analysis of drought impacts on vegetation cover and land surface temperature in the Kurdistan Region of Iraq. *Water*, 14(6), 927. <https://doi.org/10.3390/w14060927>

Guo, X., Zhang, H., Wu, Z., Zhao, J., & Zhang, Z. (2017). Comparison and evaluation of annual NDVI time series in China derived from the NOAA AVHRR LTDR and Terra MODIS MOD13C1 products. *Sensors*, 17(6), 1298. <https://doi.org/10.3390/s17061298>

Hameed, H. (2013). Water harvesting in Erbil Governorate, Kurdistan region, Iraq: detection of suitable sites using geographic information system and remote sensing. Student thesis series INES. <http://lup.lub.lu.se/student-papers/record/3737025>

Ibrahim, H. S. (2024). Analysis of Monthly Global Solar Radiation in Erbil-Iraq. *Science Journal of University of Zakho*, 12(3), 361-366. <https://doi.org/10.25271/sjuz.2024.12.3.1312> <https://doi.org/10.25271/sjuz.2024.12.3.1312>

HS, R. M. (2009). Drought climatology of Indo-Gangetic region of India using remote sensing and crop growth simulation models. <http://hdl.handle.net/10603/6265>

Jiao, W., Zhang, L., Chang, Q., Fu, D., Cen, Y., & Tong, Q. (2016). Evaluating an enhanced vegetation condition index (VCI) based on VIUPD for drought monitoring in the continental United States. *Remote Sensing*, 8(3), 224. <https://doi.org/10.3390/rs8030224>

Karim, T. H., Keya, D. R., & Amin, Z. A. (2018). Temporal and spatial variations in annual rainfall distribution in Erbil province. *Outlook on Agriculture*, 47(1), 59-67. <https://doi.org/10.1177/0030727018762968>

Kogan, F., Stark, R., Gitelson, A., Jargalsaikhan, L., Dugrajav, C., Tssoj, S. (2004). Derivation of pasture biomass in Mongolia from AVHRR-based vegetation health indices. *Int. J. Remote Sens.* 25, 2889-2896. <https://doi.org/10.1080/01431160410001697619>

Kogan, F. N. (1986). Climate constraints and trends in global grain production. *Agricultural and Forest Meteorology*, 37(2), 89-107. [https://doi.org/10.1016/0168-1923\(86\)90001-8](https://doi.org/10.1016/0168-1923(86)90001-8)

Kogan, F. N. (1990). Remote sensing of weather impacts on vegetation in non-homogeneous areas. *Int. J. Remote Sens.* 11, 1405-1419. <https://doi.org/10.1080/01431169008955102>

Leal Filho, W. (2011). Experiences of climate change adaptation in Africa. Springer. <https://doi.org/10.1007/978-3-642-22315-0>

Lee, S.-H., Yoo, S.-H., Choi, J.-Y., & Bae, S. (2017). Assessment of the impact of climate change on drought characteristics in the Hwanghae Plain, North Korea using time series SPI and SPEI: 1981-2100. *Water*, 9(8), 579. <https://doi.org/10.3390/w9080579>

Mikail, A. Q., & Hamad, R. (2023). Mapping Flood Vulnerability by Applying EBF And AHP Methods, in the Iraqi Mountain Region. *Science Journal of University of Zakho*, 11(1), 1-10. <https://doi.org/10.25271/sjuz.2023.11.1.1033>

Park, H., Kim, K., & Lee, D. K. (2019). Prediction of severe drought area based on random forest: Using satellite image and topography data. *Water*, 11(4), 705. <https://doi.org/10.3390/w11040705>

Pei, F., Wu, C., Liu, X., Li, X., Yang, K., Zhou, Y., Wang, K., Xu, L., & Xia, G. (2018). Monitoring the vegetation activity in China using vegetation health indices. *Agricultural and Forest Meteorology*, 248, 215-227. <https://doi.org/10.1016/j.agrformet.2017.10.001>

Qu, C., Hao, X., & Qu, J. J. (2019). Monitoring extreme agricultural drought over the Horn of Africa (HOA) using remote sensing measurements. *Remote Sensing*, 11(8), 902. <https://doi.org/10.3390/rs11080902>

Razvanchy, H. A. S. (2008). Modelling some of the soil properties in the Iraqi Kurdistan Region using Landsat datasets and spectroradiometer (Doctoral dissertation). Cranfield University, Cranfield, UK. <http://dx.doi.org/10.5194/isprs-archives-XLII-2-W16-21-2019>

Saeed, M. A., & Abas, K. (2012). Analysis of Climate and Drought Conditions in the Federal region of Kurdistan. *International Scientific Journal Environmental Science*, 2. <https://doi.org/10.1007/s12205-021-2046-x>

Sahoo, R., Dutta, D., Khanna, M., Kumar, N., & Bandyopadhyay, S. (2015). Drought assessment in the Dhar and Mewat Districts of India using meteorological, hydrological and remote-sensing derived indices. *Natural Hazards*, 77, 733-751. <https://doi.org/10.1007/s11069-015-1623-z>

Sholihah, R. I., Trisasongko, B. H., Shiddiq, D., La Ode, S. I., Kusdaryanto, S., & Panuju, D. R. (2016). Identification of agricultural drought extent based on vegetation health indices of landsat data: case of Subang and Karawang, Indonesia. *Procedia Environmental Sciences*, 33, 14-20. <https://doi.org/10.1016/j.proenv.2016.03.051>

Song, C., Yue, C., Zhang, W., Zhang, D., Hong, Z., & Meng, L. (2019). A remote sensing-based method for drought monitoring using the similarity between drought eigenvectors. *International Journal of Remote Sensing*, 40(23), 8838-8856. <https://doi.org/10.1080/01431161.2019.1624860>

Sun, D., & Kafatos, M. (2007). Note on the NDVI-LST relationship and the use of temperature-related drought indices over North America. *Geophysical research letters*, 34(24). <https://doi.org/10.1029/2007GL031485>

Sutcliffe, J. V. (2012). Hydrology: A Question of Balance. *Int. Water Manag. Institute*, Colombo, Sri Lanka, Spons. this Publ. 29-30. <https://www.amazon.com/Hydrology-Question-Balance-Proceedings-Reports/dp/1901502775>

UNESCO. (2009). Survey of Infiltration Karez in Northern Iraq: History and Current Status of Underground Aqueducts A report prepared for UNESCO. 56. <https://unesdoc.unesco.org/ark:/48223/pf0000185057>

UNISCO. (2014). Integrated drought risk management- DRM executive. Natl. Framew. IRAQ AN Anal. Rep. MARcH Second edi. <https://unesdoc.unesco.org/ark:/48223/pf0000228343>

USAID, I. (2008). Kurdistan Region: Economic Development Assessment. In: United States Agency for International Development Washington, DC. <https://www.usaid.gov/iraq>

Vogt, J. V., Viau, A. A., Beaudin, I., Niemeyer, S., & Somma, F. (1998). Drought monitoring from space using empirical indices and physical indicators. *Proc. Int. Symp. on Satellite-Based Observation: A Tool for the Study of the Mediterranean Basin*, Tunis, Tunisia. [http://dx.doi.org/10.1007/978-94-015-9472-1\\_13](http://dx.doi.org/10.1007/978-94-015-9472-1_13)

Walther, C. (2011). Managing Change in the Marshlands: Iraq's Critical Challenge. United Nations Integrated Water Task Force for Iraq, United Nations: Iraq. <https://doi.org/10.1063/5.0033124>

Wan, Z., Wang, P., & Li, X. (2004). Using MODIS land surface temperature and normalized difference vegetation index products for monitoring drought in the southern Great Plains, USA. *International Journal of Remote Sensing*, 25(1), 61-72. <https://doi.org/10.1080/0143116031000115328>

Wang, H., Chen, Y., Pan, Y., & Li, W. (2015). Spatial and temporal variability of drought in the arid region of China and its relationships to teleconnection indices. *Journal of hydrology*, 523, 283-296. <https://doi.org/10.1016/j.jhydrol.2015.01.055>

Wilhite, D. A., Pulwarty, R.S. (2018). Drought and Water Crises, Drought and Water Crises. <https://doi.org/10.1201/9781315265551>

Zhang, Y., Jin, J., Jiang, S., Ning, S., Zhou, Y., & Wu, Z. (2019). Quantitative assessment model for the effects of drought mitigation on regional agriculture based on an expectation index of drought mitigation effects. *Water*, 11(3), 464. <https://doi.org/10.3390/w11030464>